SINGLE-MODE OPTICALLY-ACTIVATED PHASE MODULATOR ON GaAs/GaAlAs COMPOUND SEMICONDUCTOR CHANNEL WAVEGUIDES

R. T. Chen

Microelectronics Research Center
Department of Electrical and Computer Engineering
University of Texas, Austin
Austin, TX78712

and

Dan Robinson and Robert Shih

Physical Optics Corporation
2545W 237 Street
Torrance, CA90505

ABSTRACT

We report an optically-activated phase modulator (OAM) and modulator array on GaAs-GaAlAs compound semiconductor channel waveguides. A channel waveguide device with an optical activation window of 5 μm in diameter was fabricated. Optical activation was produced by using a HeNe 632.8 nm wavelength as the free-carrier generator and a 1.3 μm laser as the signal carrier. Thirty-three percent modulation depth was observed and 10^{-2} index modulation was experimentally confirmed on an OAM working in the phase modulation regime. OAMs working in both phase- and cutoff-modulation regimes were theoretically determined by considering the fluctuation of the waveguide confinement factor. 8.2 dB modulation depth was observed on an OAM working at the cutoff regime. Furthermore, the activation source is in the mW power region which significantly reduces the size and cost of all optical switching devices.

1.0 INTRODUCTION

The first laser was built in 1960 and within a decade laser beams spanned the range from infrared to ultraviolet. The availability of high power coherent sources led to the discovery of a number of new optical effects (second harmonic generation, linear and quadratic electrooptic effects, etc.) and thus to the development of a myriad of marvelous new devices. The technology needed to produce practical optical communication devices and systems is fast evolving.

The sophisticated use of crystals in devices such as second harmonic generators, electrooptics, acoustooptics, and magneto-optics has spurred a great deal of contemporary research in crystal optics. In the early 1970's, the concept of integrating different passive and active devices, such as lasers, waveguides, modulators, detectors, lenses, and prisms, in hybrid or monolithic forms was introduced. Integrated optoelectronics is a far-reaching attempt to apply thin film and integrated electronics technology to optical circuits and devices. By means of integrated optics, one has the potential to achieve higher speeds and more economical optical communication and data processing systems. Integrated optics can also provide a more convenient interface between optical and electronic systems.

One of the major building blocks of optoelectronic integrated circuits (OEIC) is the optical guided wave modulator. The realization of optical communication and computing with high parallelity, large modulation bandwidth and low propagation loss have made the optical wave an attractive information carrier.

0-8194-0973-1/93/$4.00

Within the past fifteen years, several types of guided wave electrooptic modulators have been built. The electrooptic modulation of light can be separated into phase [1-5], polarization [6,7], intensity [8-9], and multi-quantum well (MQW) [10] modulation. The fundamental emphasis of electrooptic and all-optical modulators is focusing on changing the index of refraction of the optical and electrooptic materials within which the optical waves propagate. In this paper, an optically-activated modulator on a GaAs/GaAlAs compound semiconductor channel waveguide was successfully developed. The devices we report here can be used either as optically-enhanced phase modulators or as an optically-activated cutoff modulators. The device parameters can be designed to satisfy the criterion needed for either case.

A description of the fabrication procedure for the proposed device is described. The etching process, channel waveguide formation on the GaAs/GaAlAs substrate, optical window formation, channel waveguide edge cleavage to facilitate end-fire coupling, and device packaging are reported. Performance of the modulators and modulator arrays is detailed in Section 3. Demonstration of optically-activated phase modulators is presented first followed by considerations for waveguide design and the reporting on optically-activated modulators working at the cutoff boundary. The phase shift of the guided wave as a function of modulating optical wave (visible) is measured. Incorporation of a DC-biased voltage enhanced the modulation depth. The theoretically projected modulation speed is provided. The ultimate limitation on the speed of this type of device is the free carrier lifetime of the semiconductor material involved. This is similar to counterpart microwave devices. For undoped GaAs the carrier lifetime is around 10 ns [11]. Carrier lifetime in picosecond to subpicosecond range has been achieved in GaAs by using doping or ion implantation techniques [12,13]. The results demonstrate that device length even shorter than for multiple quantum well devices is enough to provide a high extinction ratio for the optical throughput of the modulator. Depending on the application scenario, both all-optical and electrooptic modulators are realizable. Finally, concluding remarks are made in Section 4.

2.0 Device Fabrication

GaAs provides a direct band gap, high electron and hole mobilities, and semi-insulating substrates. The combination of these characteristics allows us to make high speed, monolithic, optoelectronic integrated circuits. Optical waves of any light with wavelengths within the 0.9 to 5 μm range can be used as the signal carrier. Optical photons from both coherent and incoherent light sources with $h\nu > E_g$ (i.e., energy gap of GaAs waveguides) can be employed as the source for activating a vast number of free electrons and holes. The basic structure for the single-channel optically-activated modulator (OAM) on a GaAs-GaAlAs waveguide is shown in Figure 1. The small circular window area within the electrode pad is designed to input the optical photons with $h\nu > E_g$ to generate free electron and hole pairs. The optical wave representing the signal carrier can be coupled into the waveguide through end-firing or by a grating. A reverse bias (if needed) can be added across the Schottky barrier to form a depletion region to accelerate the free carriers.

A single-mode optically-activated modulator and a linear array of identical modulators have been successfully fabricated. First, a planar GaAs-GaAlAs heterostructure with an aluminum concentration of approximately 7% was grown on an x-cut N^+ substrate using a MOCVD system [14]. Planar waveguide formation was first confirmed experimentally through end-fire coupling. The channel waveguide and waveguide array were made through the conventional lithographic process. AZ1400 photoresist was employed as the masking material during the wet etching process which consisted of HCl, H_2O_2, and H_2O in the ratio of 80:4:1, and provided an etching rate of 1.1 μm/min at room temperature. After the channel waveguide was empirically verified to be a successful optical guide, a thin Al film was deposited on the waveguide surface. A lift-off technique was employed to form the desired window for optical activation. A circular window 5 μm in diameter was formed on top of the channel waveguide. The microstructure revealed by a microscope is shown in Figure 2. A key portion of the setup is detailed in Figure 2 where the area of interaction is clearly indicated. The window area is located right on top of the GaAs channel

waveguide within which the 1.3 μm laser light is propagating. The optical activation source can be introduced by using either an imaging lens (Figure 1) or a single-mode fiber (not shown). The channel waveguide, Al electrode and the 5 μm diameter window are clearly displayed. The parameters and waveguide orientations for both the basic modulator and the modulator array are given in Table 1. Finally, after formation of an ohmic contact on the bottom face of the specimen, both end faces of the device were cleaved to facilitate edge coupling for subsequent experiments. Figure 3 shows the photograph of one of the cleaved end faces of the modulator array. The finished sample was then mounted on a special IC chip and placed in a device holder for detailed experimentation. The device package is shown in Figure 4. Bonding wires, chip carrier, GaAs OAM, 50 Ω microstrip line and SMA connectors are clearly shown.

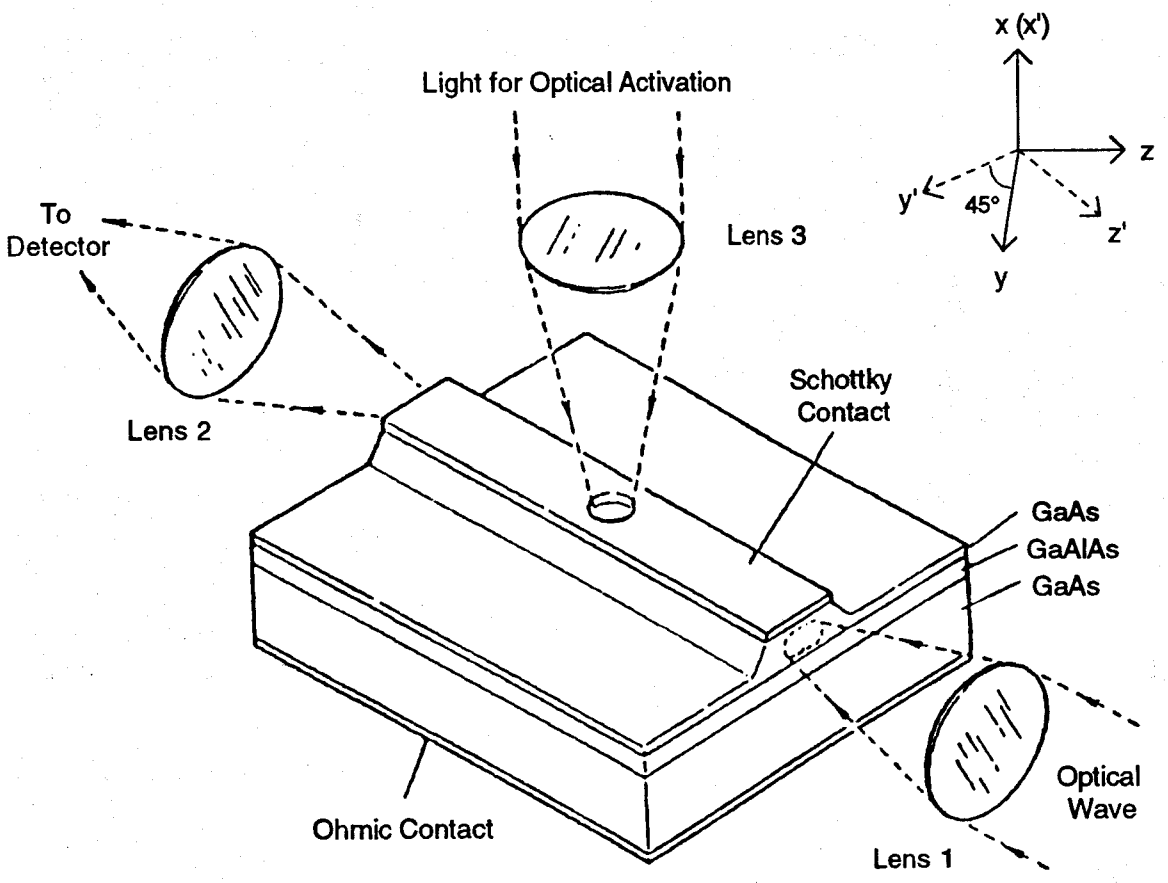

Figure 1
Basic Structure of Optically-Activated Modulator on GaAs

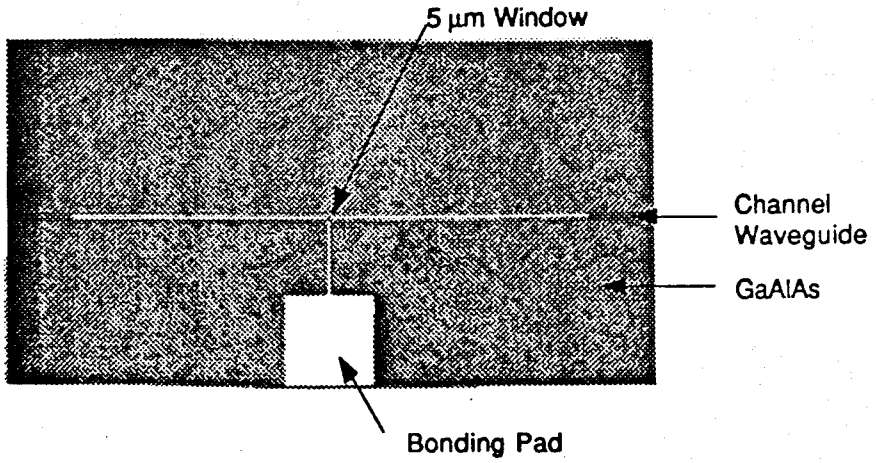

Figure 2
0.5 mm Electrode on a GaAs/GaAlAs Channel Waveguide and 5 μm Diameter Window for Optical Activation on a Single-Mode GaAs/GaAlAs Channel Waveguide

Table 1. Waveguide Dimensions and Orientations of GaAs/GaAlAs Channel Waveguide Optically-Activated Modulator and Modulator Array

Common Parameters:	
Channel Width	5 μm
Channel Depth	1 to 1.5 μm
Waveguide Type	Ridge Channel
Etching Solution	$HCl:H_2O_2:H_2O$ = 80:4:1
GaAlAs Thickness	1 μm
Al Concentration	7 percent
Schottky Contact	Al 5000 Å thick
Substrate Orientation	(100)
Waveguide Direction	[011]
Window Size (Interaction Length)	5 μm in diameter
Cutoff Modulator Array:	
Separation Between Adjacent Channels	20 μm
Area of Bonding Pad	4 mil. x 4 mil.
No. of Channels	10
Packing Density	500 channels/cm

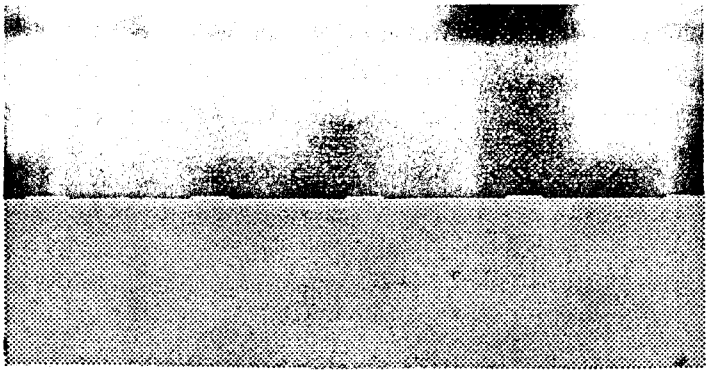

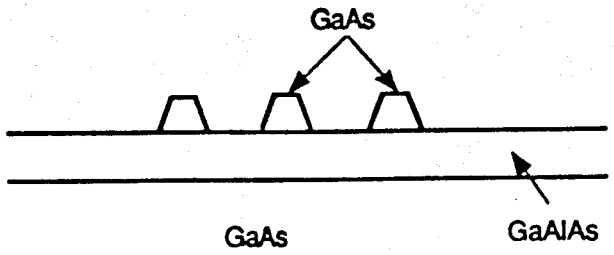

Figure 3
Illustration of One of the Cleaved End Faces of the Modulator Array

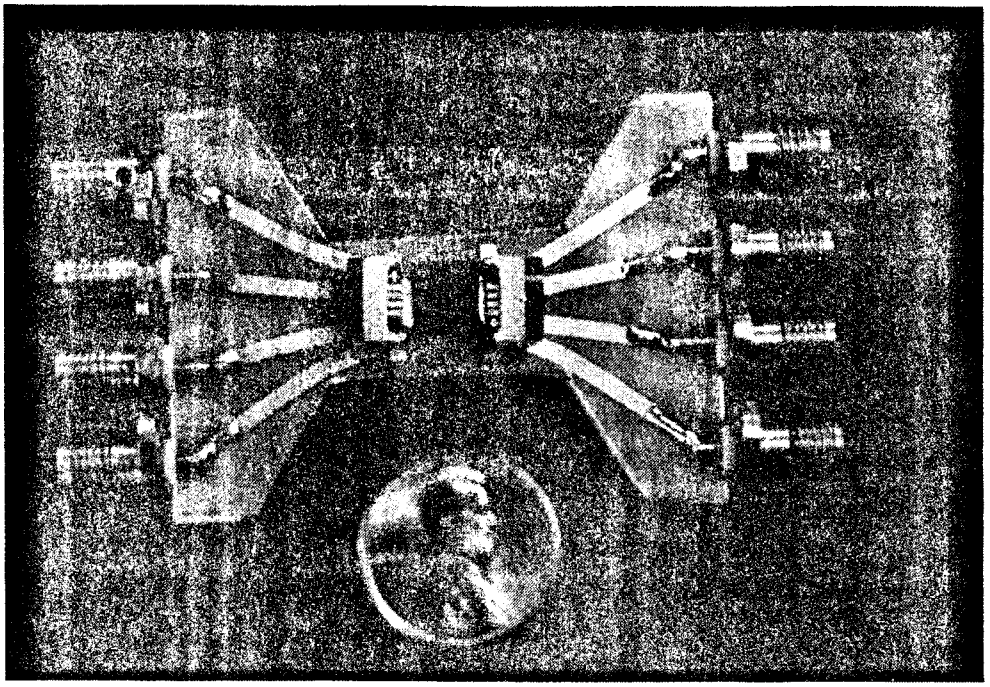

Figure 4
Fully Packaged Optically-Activated Modulator (OAM) on
GaAs-GaAlAs Channel Waveguide

3.0 PERFORMANCE OF THE MODULATOR AND THE MODULATOR ARRAY

In this section, the experimental results are presented. The setup employed to do the all-optical and the electrooptic measurement is described first. An optically-activated modulator working in the phase modulator regime (well above the cutoff boundary) was produced. The feasibility of using the same device with a 0.5 mm electrode (Figure 2) as a linear electrooptic modulator is also introduced. Theoretical calculation was conducted using the confinement factor as an indicator to determine device criterion suitable for either the phase- or cutoff-regime. The result of the calculation is summarized in Section 3.3. Further results of the optically-activated and electrooptic cutoff modulator is reported in Section 3.4.

3.1 Experimental Setup

The setup employed for the demonstration is shown in Figure 5 where the optical activation source (0.632 μm HeNe), 1.3 μm laser diode, GaAs/GaAlAs channel waveguide modulator package, coupling and imaging lenses, Ge photodetector (PIN) and the signal generator are clearly shown. The coupling lens provides a diffraction-limited beam waist at the input edge of the waveguide OAM. The imaging lens transfers the near field image of the throughput light from the channel waveguide to the detector. A near field image of the guided wave (1.3 μm) taken by a vidicon camera is illustrated in Figure 6. The background noise was filtered out after the Fourier transform lens. Modulation of the device is observed through the oscilloscope.

3.2 Optically-Activated Phase Modulator

The first device we demonstrated was a single-mode optically-activated phase modulator. By shining the HeNe 0.632 μm on the 5 μm diameter window area, we generated a 33% modulation depth. The results we demonstrated provide us with not only a new GaAs waveguide device but also a device interaction length compatible or even shorter than that of MQW devices (~100 μm).

For a Fabry-Perot phase modulator, the existence of loss reduces the peak transmission to less than unity. Figure 7 shows the curves of I_t/I_i with different propagation loss as a parameter. The reflectance R is set at 30%, which is the case at the GaAs/air interface. It is clear that to increase the device modulation depth, the GaAs/GaAlAs waveguide propagation loss should be reduced to a minimum value. It is obvious that the effective index modulation, i.e., Δn_{eff}, due to optical activation can be found by measuring the T value. The optically-activated modulation is shown in Figure 8. The top trace is the HeNe 0.633 μm modulating light source and the bottom trace the modulated guided wave (1.3 μm) which was end-fire coupled into the channel waveguide. Modulation depth to 33% was observed for a GaAs waveguide with 0.4 dB/cm propagation loss. A similar result was also observed in a Mach-Zehnder interferometer [15]. It is clear that in order to increase the throughput intensity, waveguide propagation loss needs to be minimized. Figure 9 shows the measured phase shift as a function of the intensity of the optical activation. To compare the optically-activated modulation with a linear electrooptic phase modulator, an AC electrical field was added to the electrode. The experimental results in Figure 10 show that in order to generate the same T value (33% in this case), we need to have a linear electrooptic device with 1 mm interaction length and 10 volt applied voltage. The interaction length is 200 times longer than the linear dimension of the window of the optically-activated modulator. Such compactness significantly enhances the packing density of the modulator array. Note that the modulation depth of 33% corresponds to ~55° phase shift. If the optical window is enlarged to 15 μm, the maximum value of T will be generated.

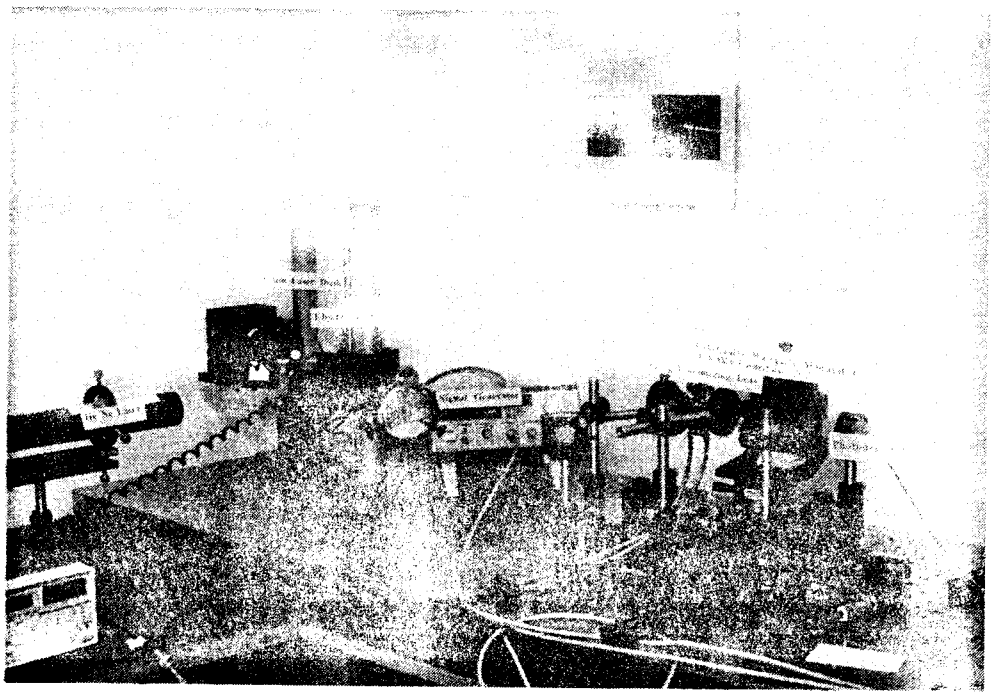

Figure 5
Setup for OAM on GaAs/GaAlAs Channel Waveguide

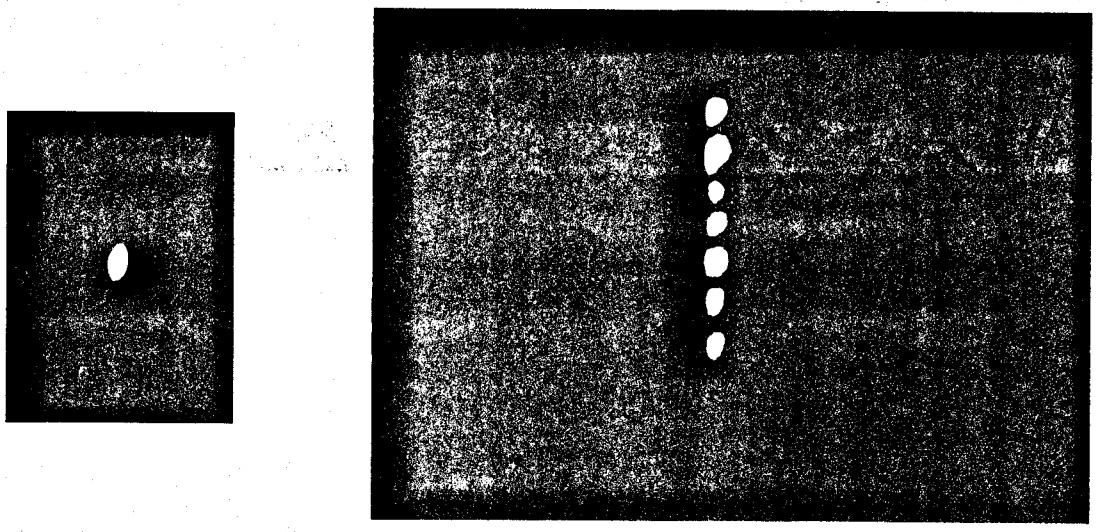

(a) (b)

Figure 6
Near-Field Pattern of the Single-Mode Guided Wave from GaAs/GaAlAs Channel Waveguide. (a) Single-Channel and (b) Channel Waveguide Array.

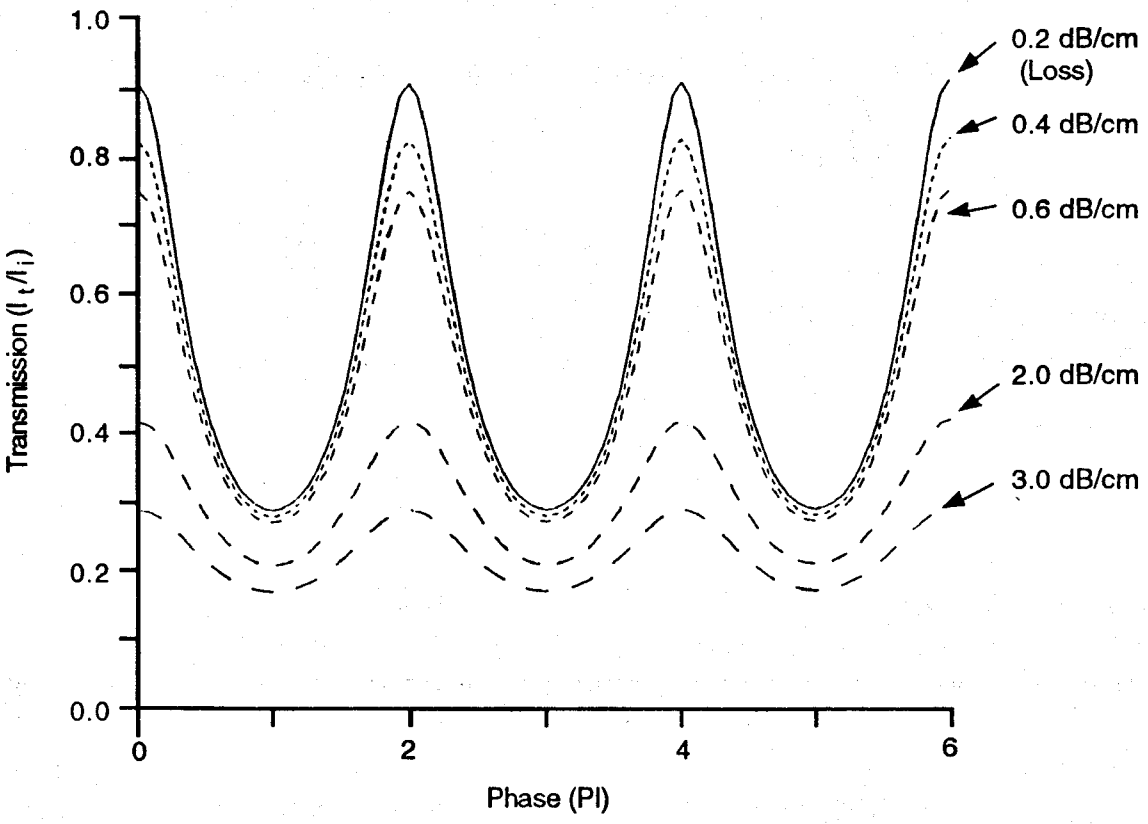

Figure 7
Transmission (I_t/I_i) of the GaAs OAM as a Function of Phase Shift with Waveguide Propagation Loss as a Parameter

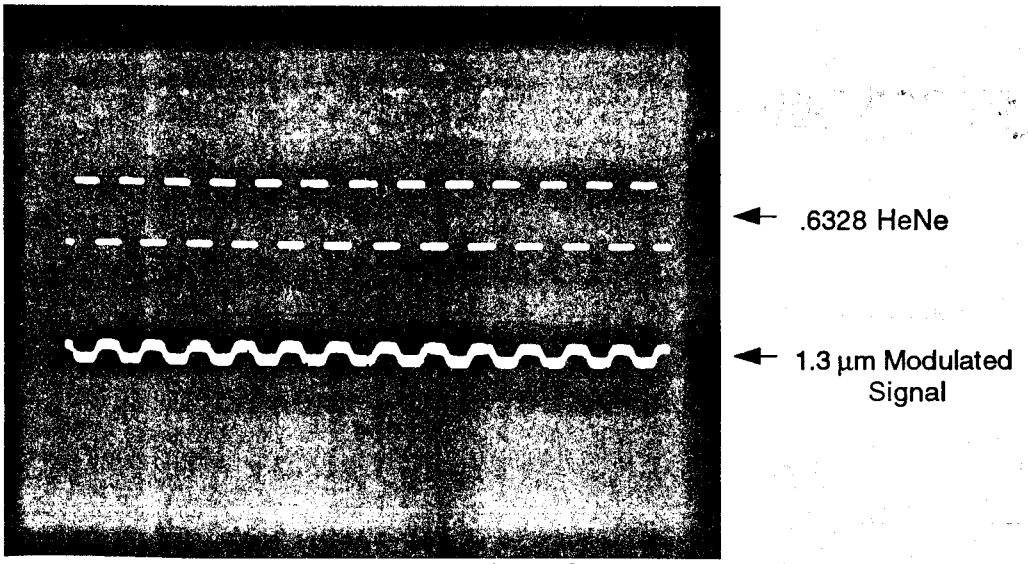

Figure 8
Optically-Activated Modulator: Top Trace = 0.633 µm Modulating Light Source, Bottom Trace = Modulated 1.3 µm Guided Wave (Modulation Speed 4 kHz)

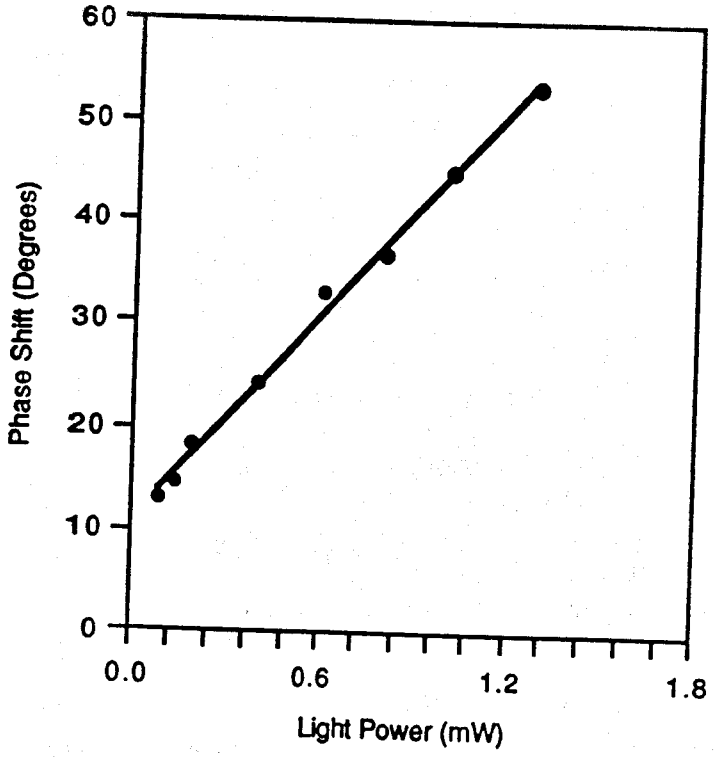

Figure 9
Photo-Induced Phase Shift in the Guided Light Versus Modulating Light Power with Interaction Length of 5 μm

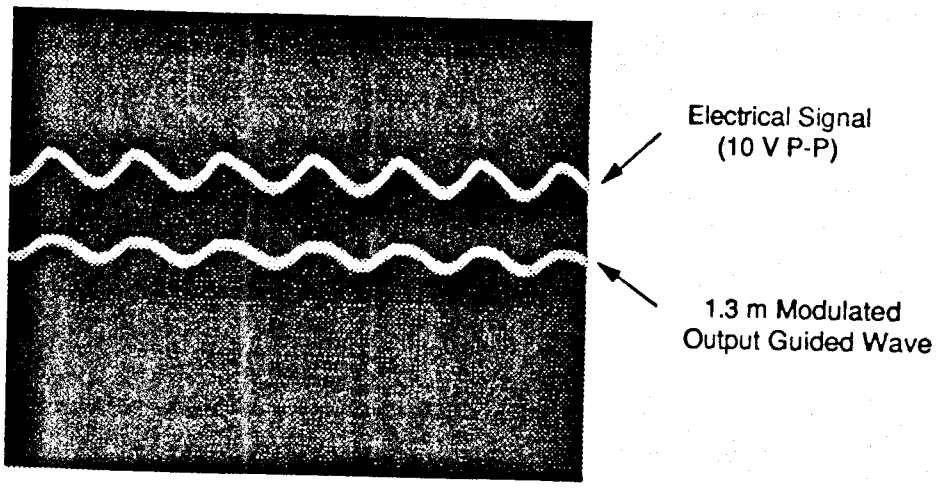

Figure 10
33% Modulation Depth of the 1.3 μm Guided Wave Throughput Generated Directly from a 0.5 mm Electrode with 10 Volt Peak to Peak Value at 4 kHz

There are three sources of modulation which can be used in the waveguide modulator. They are: 1) direct modulation of the 1.3 μm laser diode by varying the current of the laser diode driver, 2) optical activation using the 0.632 μm HeNe laser, and 3) electrical signal applied directly onto the Schottky contact located on top of the channel waveguide (Figure 2). Combinations of these modulation mechanisms were tried and the results are shown in Figure 11. Note that the combination of these modulation outputs is shown in the bottom trace of the photograph.

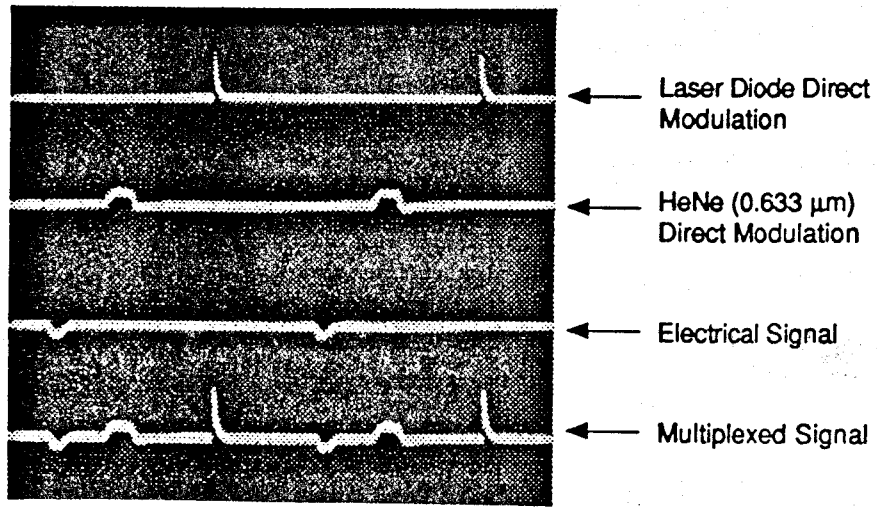

Figure 11
Detection of the 1.3 μm Output Signal from the GaAs Channel Waveguide. Multiplexing of These Three Signals are Shown. The Modulation Frequency is Fixed at 4 kHz.

3.3 Waveguide Design Considerations

Experimental results we observed show that the optically-activated modulator (OAM) can work either as a Fabry-Perot phase modulator or a cutoff modulator. Both the phase modulator and the cutoff modulator are single-mode devices which use the same electrode structure. The difference between them is that the optically-activated phase modulator is well above the cutoff condition so that the confinement factor C_f, which is defined as

$$C_f = \frac{\left|\langle W|W\rangle\right|_{\text{guiding region}}}{\left|\langle W|W\rangle\right|_{\text{guiding region}} + \left|\langle W|W\rangle\right|_{\text{cladding regions}}}, \qquad (1)$$

is not changed significantly by the existence of an external bias field. In Eq. (1), $|W\rangle$ is the electric field distribution function of the guided mode. In the case of an optically-activated modulator working in the cutoff regime, however, the confinement factor and thus waveguide propagation loss changes drastically

due to the existence of an external electric field. The sensitivity of the waveguide confinement factor C_f to the existence of an applied electric field is a major parameter in determining the waveguide's suitability for use as either a phase or a cutoff modulator.

In order to clarify this statement, a theoretical calculation was made to evaluate the influence of the waveguide's effective index on the confinement factor. The experimental results imply that a good optically-activated cutoff modulator is achieved by a waveguide with effective index very close to the substrate index. Therefore, it is essential that the waveguide effective index be in the neighborhood of the cutoff boundary. The small variation of the effective index can be induced by either an external voltage or a small perturbation of such waveguide parameters as aluminum concentration or waveguide dimension.

The channel waveguide used was the subject of calculation. It was found that only the evanescent tail penetrating into the GaAlAs cladding layer was changed significantly. A three-dimensional surface plot with effective index as the x-axis, the distance of the waveguide in the depth direction as the y-axis (origin at the center of the GaAs guiding layer), and the electric field of the guided mode as the z-axis, is shown in Figure 12. The refractive index of $Ga_{0.93}Al_{0.07}As$ is 3.3710 at 1.3 μm. The waveguide depth is varied in

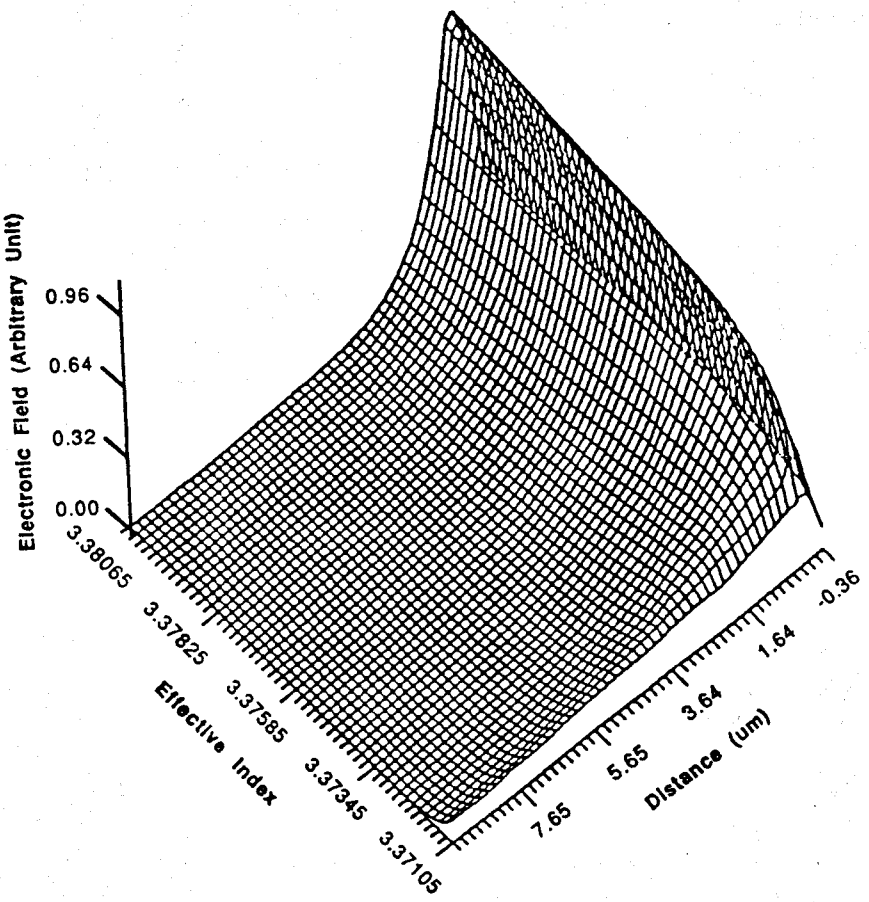

Figure 12
Propagating Mode Profiles Along the Transverse Direction of the GaAs Waveguide (GaAs-$Ga_{0.93}Al_{0.07}As$). The Increase of the Evanescent Wave is Clearly Seen.

the neighborhood of 1 μm. The theoretical calculation shows that, when the effective index is very close to 3.3710, the evanescent tail of the guided wave penetrating into the $Ga_{0.93}Al_{0.07}As$ cladding layer is the major reason for the decrease of the confinement factor. The peak of the electric field clearly decreases as the guided mode index moves closer to the cutoff boundary. Each of the waveguide propagating mode profiles shown in Figure 12 is normalized so that

$$\left|\langle W|W\rangle\right| = 1 \qquad (2)$$

where $|W\rangle$ is the waveguide mode function and the integration covers all of the area. The equal electric field lines of the various propagating modes corresponding to Figure 12 are shown in Figure 13. The increase of the intensity of the evanescent tail as the effective index of the guided mode moves closer to 3.3710 is clearly shown in this figure. The resulting confinement factor, as defined by Eq. (2), is a function of the guided wave mode index, as shown in Figure 14. The confinement factor drops to zero as N_{eff} shifts to the value of the cladding index. Two regions are evident in Figures 12 and 14. The first region represents the waveguide domain suitable for a cutoff modulator where the confinement factor changes drastically as a function of the effective index, N_{eff}. The second region is the waveguide domain, suitable for a phase modulator, where the confinement factor changes slightly under the influence of an external activation source. It is clearly shown in these figures that the dynamic range of the waveguide effective index appropriate for an optically-activated phase modulator is larger than that of an optically-activated cutoff modulator.

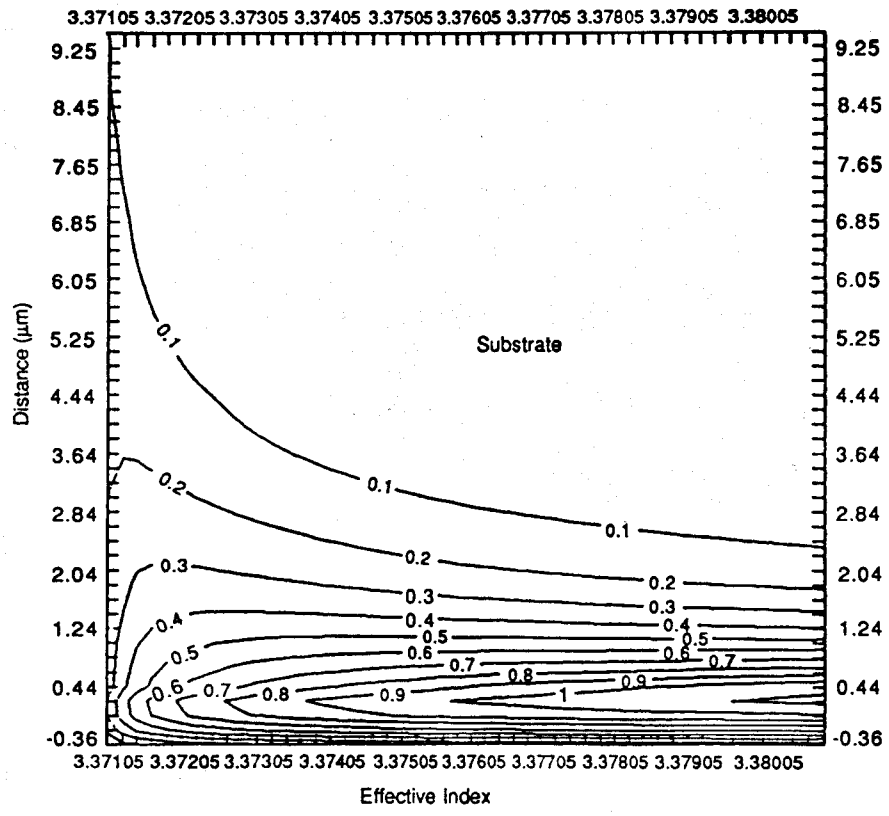

Figure 13
Equal Electrical Field Topology of the Propagating Modes of the GaAs Waveguide (GaAs-$Ga_{0.93}Al_{0.07}As$) Corresponding to Figure 13

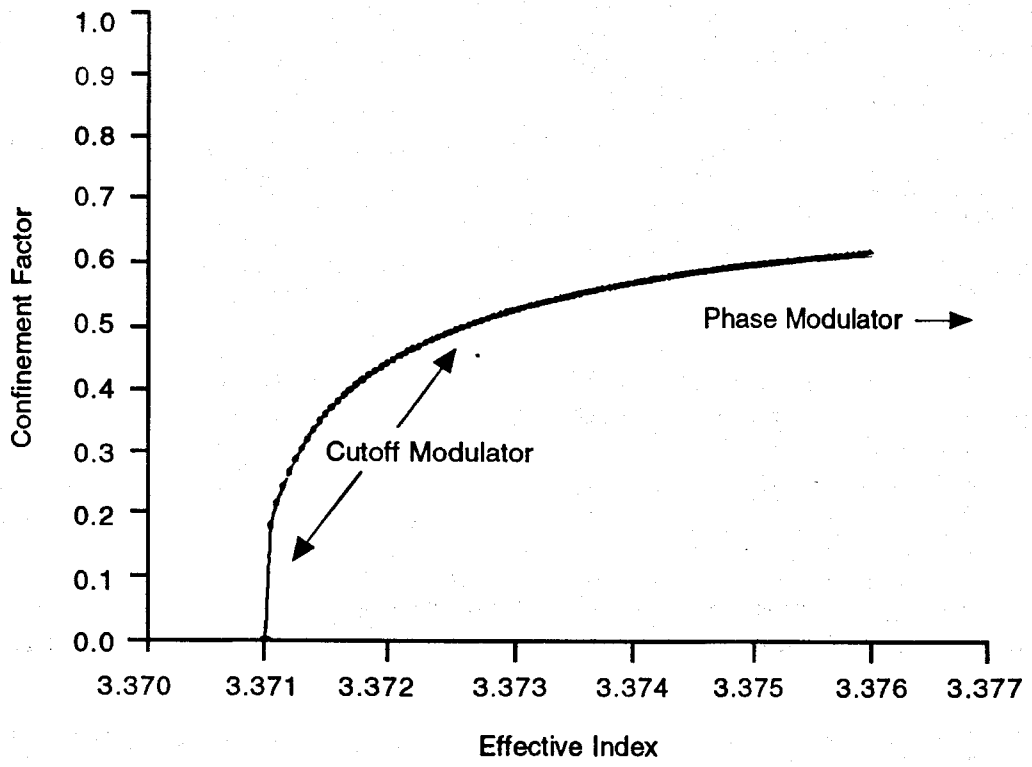

Figure 14
Confinement Factors as a Function of Effective Indices of the GaAs Waveguide (GaAs-$Ga_{0.93}Al_{0.07}As$)

3.4 Optically-Activated Cutoff Modulator

Based on the discussion presented in Section 3.3, a single-mode GaAs-GaAlAs channel waveguide with an effective index closer to the cutoff boundary was tested. The device we tested in this section has a narrower waveguide dimension and is thus closer to the cutoff boundary (Figure 14). The rest of the setup is the same as that shown in Figure 5. Operation of the device can be carried out either by shining DC HeNe laser light on the window area and applying the AC signal through the SMA injection port (Figure 4) or by directly encoding the modulated signal onto the HeNe laser. Figure 15 shows the optically-activated modulation by directly modulating the HeNe laser with an electrical chopper. The top trace of the figure is the HeNe laser light and the bottom trace the IR throughput from the GaAs channel waveguide. A modulation depth of 8.5 dB was measured. Note that the device was biased at -12 volts. The existence of a DC bias voltage significantly enhanced the current effect. Optical activation through current modulation is not polarization-dependent. As a result, both TE and TM modes demonstrated a large magnification of the IR guided wave throughput signal.

With respect to the modulation speed of the GaAs/GaAlAs channel waveguide OAM, the first limiting factor is the free carrier lifetime of the semiconductor material. For undoped GaAs, the carrier lifetime is around 10 ns [11]. Carrier lifetime in the picosecond and subpicosecond range has been achieved in GaAs by using doping or ion implantation techniques [12,13]. As a result of this achievement, the other limiting factor -- parasitic RLC factors [25] associated with electronic lumped structures -- shall be considered.

A computer simulation was made to evaluate the voltage response as a function of the input rf frequency. The results are shown in Figure 16. Figure 16(a) and (b) represent the two extreme cases with the related parameters as shown.

As far as the lifetime of the optically generated free carriers is concerned, carrier lifetime in the picosecond to subpicosecond range was achieved in GaAs by using doping and ion implantation techniques [12,13]. Accordingly, the modulation speed is not limited by the current effect.

4.0 CONCLUSIONS

We present for the first time, to the best of our knowledge, an optically-activated phase modulator (OAM) on a GaAs/GaAlAs heterostructure channel waveguide. Experimental results show that a device interaction length shorter than that of MQWs is capable of producing an OAM device with 8.2 dB modulation depth. Theoretical calculations are provided to compare the index modulation between optical activation and the linear electrooptic effect. Experimental work was also conducted to confirm the magnitude of the optically-generated index modulation through free-carrier injection. A single-mode GaAs OAM device can be designed either as a phase modulator or as a cutoff modulator. A theoretical calculation based on the variation of the confinement factor as a function of the guided mode effective index is provided. Design criterion for both cases is given. Optically-activated modulators using GaAs/GaAlAs channel waveguides were fabricated. Fully packaged devices were demonstrated for both single-channel OAMs and OAM arrays. Optically-activated modulation was demonstrated in both phase modulation and cutoff modulation regimes. Signal multiplexing was further conducted using optical activation sources, IR signal carriers and electrical signals. The modulation speed/bandwidth was also considered and the results showed a multi-Gigahertz device operational bandwidth. Improvement of modulation speed is feasible by employing a traveling wave electrode structure on a semi-insulating substrate.

This research was currently sponsored by AFOSR and SDIO.

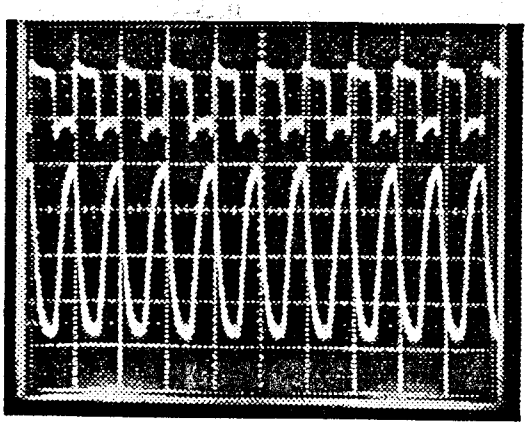

Figure 15
Optically-Activated Modulation (Bottom Trace) by Pulsing the Activation Light (Top Trace).
Modulation Frequency 4 kHz.

(a)

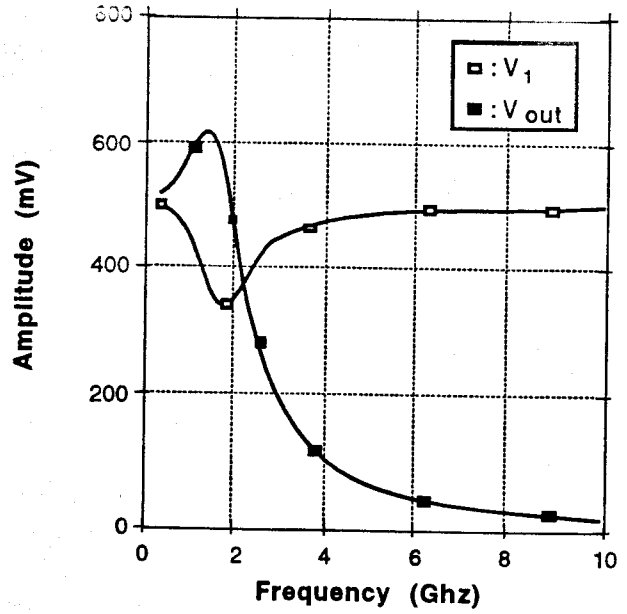

R_1 (Ohm)	L_1 (nH)	R_2 (Ohm)	L_2 (nH)	C_s (pF)
0.035	3.86	0.39	3.86	1.1

(a)

(b)

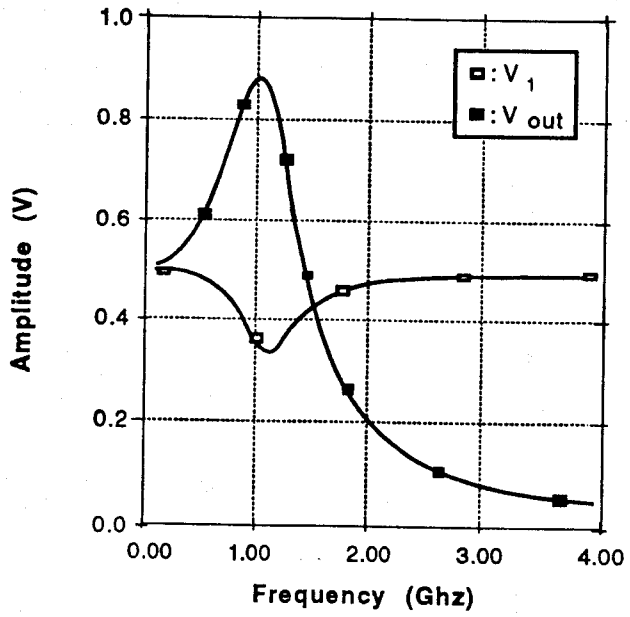

R_1 (Ohm)	L_1 (nH)	R_2 (Ohm)	L_2 (nH)	C_s (pF)
0.070	9.10	0.42	9.10	1.1

(b)

Figure 16
Computer Simulated Results of the Voltage Transfer Function of the Equivalent Circuit Shown in Figure 15 (V_1 and V_{out} are Defined in Figure 15(b))

5.0 REFERENCES

1. M. Papuchon, et al., "Electrically Switched Optical Directional Coupler: Cobra," Appl. Phys. Lett., 27, 289 (1975).
2. R. C. Alferness, R. V. Schmidt, and E. H. Tuner, "Characterization of Ti-Diffused $LiNbO_3$ Optical Directional Couplers, Appl. Opt., 18, 4012 (1979).
3. W. E. Marin, "A New Waveguide Switch/Modulator for Integrated Optics," Appl. Phys. Lett., 32, 562 (1975).
4. V. Ramaswamy, M. D. Divino, and R. D. Standley, "Balanced Bridge Modulator Switching Using Ti-Diffused $LiNbO_3$ Strip Waveguides," Appl. Phys. Lett., 32, 644-646 (1978).
5. C. L. Chang and C. S. Tsai, "Electrooptic Analog-to-Digital Convertor Using Channel Waveguide Fabry-Perot Modulator Array," Appl. Phys. Lett., 43, 22 (1983).
6. S. Y. Wang, S. H. Lin, and M. Huong, "GaAs Traveling-Wave Polarization Electro-Optic Waveguide Modulator with Bandwidth in Excess of 20 GHz at 1.3 μm," Appl. Phys. Lett., 51, 83 (1987).
7. R. T. Chen, "E-O Depolarization Switch on Y-Cut $LiNbO_3$ PE Channel Waveguides," Appl. Phys. Lett., 54, 2628 (1989).
8. R. Chen and C. S. Tsai, "Thermally Annealed Single-Mode Proton-Exchanged Channel Waveguide Cut Off Modulator," Opt. Lett., 11, 546 (1986).
9. R. Chen, "Thermally Annealed Mode Annihilation Switching Array on Proton Exchanged $LiNbO_3$ Channel Waveguides," SPIE, San Diego, CA, 1989.
10. R. Chen, et al., "GaAs-GaAlAs Heterostructure Single-Mode Channel Waveguide Cutoff Modulator and Modulator Array," IEEE J. of Quantum Electron., QE-23, 2205 (1987).
11. S. M. Sze, Physics of Semiconductor Devices, 2nd ed., p. 851 (John Wiley & Sons, 1981).
12. See, for example, D. H. Auston, Appl. Phys. Lett., 26, 101 (1975); J. A. Buck, K. K. Li, and J. R. Whinnery, J. of Applied Physics, 51, 769 (1980); P. Cheung, et al., IEEE Trans Microwave Theory and Tech., 38, 586 (1990); and C. H. Lee, IEEE Trans Microwave Theory and Tech., 38, 596 (1990).
13. M. B. Johnson and T. C. McGill, Appl. Phys. Lett., 54, 2424 (1989).
14. R. A. Soref and B. R. Bennett, "Electro-Optic Effects in Silicon," IEEE J. of Quantum Electron., QE-23, 123 (1987).
15. Z. Y. Cheng and C. S. Tsai, "Optically Activated Integrated Optic Mach-Zehnder Interferometer on GaAs," Appl. Phys. Lett., 59, 18, 2222 (1991).
16. "Lead Inductance Comparisons," Semiconductor International, 74 (June 1988).